Journal of Alloys and Compounds 509 (2011) 4201–4204

Contents lists available at ScienceDirect

Journal of Alloys and Compounds

journal homepage: www.elsevier.com/locate/jallcom

Photoluminescence analysis of $Cd_{0.8}Mn_{0.2}Te$ single crystal grown by the vertical Bridgman method

Jijun Zhang*, Linjun Wang, Jiahua Min, Jian Huang, Kaifeng Qin, Xiaoyan Liang, Ke Tang, Lan Peng

School of Materials Science and Engineering, Shanghai University, Shanghai 200072, PR China

ARTICLE INFO

Article history:
Received 3 September 2010
Received in revised form 5 January 2011
Accepted 8 January 2011
Available online 14 January 2011

PACS:
78.55.Et
81.10.Fq

Keywords:
Semiconductors
Crystal growth
Recombination and trapping
Luminescence

ABSTRACT

In this paper, the photoluminescence (PL) spectra were detected to characterize $Cd_{0.8}Mn_{0.2}Te$ crystals grown by the vertical Bridgman method. Several monocrystalline (1 1 1) face plates with dimension of $30 \times 40 \times 2\ mm^3$ were sliced from the as-grown $Cd_{0.8}Mn_{0.2}Te$ ingot, where the PL analysis was conducted. The PL spectra revealed the neutral acceptor bound exciton (A^0, X) peaks and the donor–acceptor pair (DAP) peaks. The activation energies derived from the temperature-dependent PL quenching of the (A^0, X) peak was estimated to be 5.3 meV and 45.8 meV, which suggested the binding energy of excitons to acceptors at lower temperatures and the Auger recombination at higher temperatures. A relationship for the bandgap energy of $Cd_{0.8}Mn_{0.2}Te$ as a function of temperature ranging from 10 K to 300 K was obtained. The composition uniformity of the (1 1 1) face $Cd_{0.8}Mn_{0.2}Te$ plates were analyzed with PL spectra, which shown that the variation of Mn concentration is within 0.012 mole fraction.

1. Introduction

The ternary compound $Cd_{1-x}Mn_xTe$ is a typical diluted magnetic semiconductor (DMS) known to adopt the zincblende structure with $0 < x < 0.77$ [1]. Owing to its unique magnetic and magneto-optic properties, $Cd_{1-x}Mn_xTe$ is used in many device applications, such as Faraday rotators, optical isolators and magnetic field sensors [2–4]. Recently, it is shown that $Cd_{1-x}Mn_xTe$ is a promising room temperature semiconductor detector material replacing $Cd_{1-x}Zn_xTe$ [5,6]. In comparison with $Cd_{1-x}Zn_xTe$, the bandgap of $Cd_{1-x}Mn_xTe$ is more sensitive to Mn content, therefore, less Mn content is added for the same bandgap in the range 1.7–2.2 eV which is required for optimal signal-to-noise ratio in radiation detectors [7]. The segregation coefficient of Zn in CdTe is 1.3 that high compositional variation is inevitable in $Cd_{1-x}Zn_xTe$ [8]. Meanwhile, the segregation coefficient of Mn in CdTe is close to unit so that the uniform Mn distribution is expected in entire $Cd_{1-x}Mn_xTe$ ingots [9]. For all these applications, $Cd_{1-x}Mn_xTe$ bulk crystals with high crystalline perfection are required. The $Cd_{1-x}Mn_xTe$ crystals have been grown from melt with different growth methods, such as vertical gradient freeze method, traveling heater method, and vertical Bridgman method [10–12]. However, it is revealed that the growth of high perfection, twin-free, and large size $Cd_{1-x}Mn_xTe$ single crystal remains an unresolved obstacle, mainly due to its inherent physical properties.

Photoluminescence (PL) spectroscopy is a sensitive, non-contact and non-destructive tool, suitable to characterize point defects (donors, acceptors and native defects), structural quality, and bandgap energy in $Cd_{1-x}Zn_xTe$ crystal [13–15]. PL emission spectrum depends on temperature, which is helpful for measuring activation energies of defects and understanding different types of recombination processes. The field-induced exchange effects in $Cd_{1-x}Mn_xTe$ as DMS were fully explored by the PL spectrum, and the special PL bands were defined [16,17].

In this paper, we present the PL study results of $Cd_{1-x}Mn_xTe$ ($x = 0.2$) crystals grown by the vertical Bridgman method, corresponding to the radiation detector application. The crystallinity and homogeneity of the as-grown crystal were evaluated. The temperature dependence of exciton bound PL transition and the bandgap energy in $Cd_{0.8}Mn_{0.2}Te$ crystal were analyzed.

2. Experimental

$Cd_{0.8}Mn_{0.2}Te$ (CMT) single crystals were grown by the vertical Bridgman method. High-purity raw materials of Cd (7N), Te (7N) and Mn (5N) were adopted to prevent impurities. The following steps were utilized in the crystal growth. First, the raw materials were vacuum-sealed in a carbon-coated quartz ampoule and synthesized homogeneously at 1400 K in a home-built rocking furnace for 48 h to form polycrystalline ingot. The crystal growth was then carried out in a five-zone furnace at the growth rate of 1.0 mm/h and the temperature gradient of 13 K/cm. After the solidification was completed, the crystal was in situ annealed at 1173 K for

* Corresponding author. Tel.: +86 21 56331715; fax: +86 21 56333514.
E-mail address: zhangjijun222@shu.edu.cn (J. Zhang).

0925-8388/$ – see front matter © 2011 Elsevier B.V. All rights reserved.
doi:10.1016/j.jallcom.2011.01.055

several days and finally was slowly cooled down to room temperature. The as-grown 30 mm diameter CMT crystal had lamellar twins which run parallel to the growth axis of the ingot, and several monocrystalline (1 1 1) face plates with dimension of $30 \times 40 \times 2\,mm^3$ were obtained, as shown in Fig. 1. The $10 \times 10 \times 2\,mm^3$ CMT samples were sliced from the (1 1 1) face plates for PL analysis.

Before PL measurements, all CMT samples were mechanically polished with 0.05-μm MgO suspension and then chemically polished in 2% bromine–methanol solution for 4 min, which ensured that the surface layers were removed completely. In the PL measurements, the samples were attached on a cold copper finger in a closed-cycle cryostat with grease to keep the sample temperature ranging from 10 K to 300 K. An argon ion laser with the wavelength of 488 nm was used to excite the PL spectrum. A Triax (Longjumeau, Cedex, France) 550 tri-grating monochromator with a photomultiplier, with a spectral resolution of 0.3 nm, was used to collect and to analyze the signals emitted from the samples.

3. Results and discussion

A typical temperature-dependent PL spectrum for CMT is shown in Fig. 2. Considering the origin of the emission lines, the PL spectra can be divided in three regions: (a) the exciton region, for energy higher than 1.85 eV, (b) the donor–acceptor pair (DAP) recombination, from 1.70 eV to 1.85 eV, and (c) emission at band energy <1.70 eV associated with crystal imperfections and deeper impurity levels. The main PL line is assigned to the recombination of excitons bound to the neutral acceptors, which denoted by (A^0, X). The intensity of the (A^0, X) drastically decreases upon annealing under Cd-saturated atmosphere, which suggest that the (A^0, X) line maybe related to the recombination of excitons trapped at Cd vacancies complex [18]. The parameters of the PL spectrum of CMT at 10 K shows that the (A^0, X) peak centers at 1.8836 eV, the DAP peak centers at 1.7932 eV, the full width at half maximum (FWHM) of the (A^0, X) peak Δ_{AX} is 10.7 meV, and the intensity ratio of the DAP peak and the (A^0, X) peak defined as the defect radiative density ρ is 0.081. The smaller Δ_{AX} and ρ values imply the better crystal quality [19]. We noticed that the PL spectrum of Fig. 2 do not show any emission for the band energy <1.70 eV, which also proves a relative high crystalline quality and purity of the as-grown ingot.

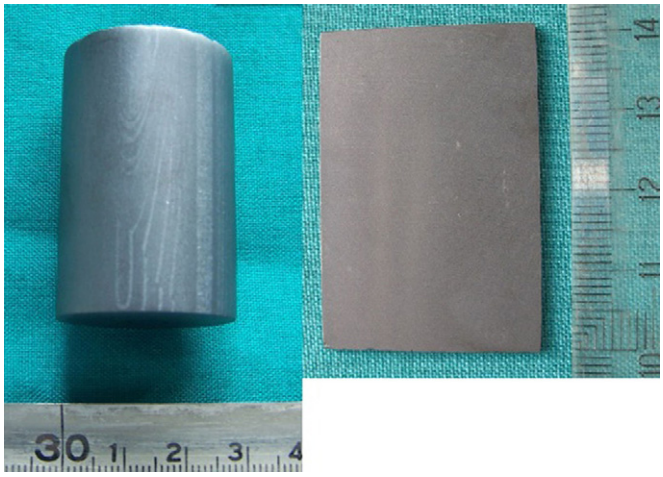

Fig. 1. Photograph of the ϕ30 mm $Cd_{0.8}Mn_{0.2}Te$ ingot, and the (1 1 1) face wafer with dimension of $30 \times 40 \times 2\,mm^3$ cut from the ingot.

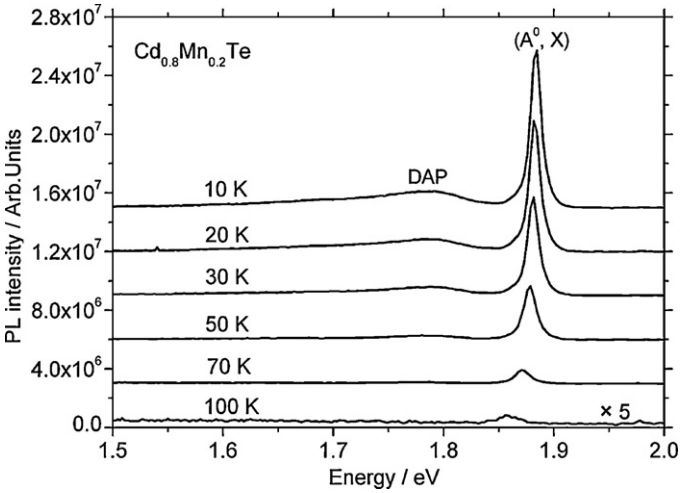

Fig. 2. Temperature dependent PL spectra of the $Cd_{0.8}Mn_{0.2}Te$ sample.

In general, additional insight regarding the nature of bands in PL spectra can be obtained by studying how the spectrum evolves with changing temperature, which is the PL quenching process. From the PL spectra in Fig. 2, as the temperature is increased, the luminescence of both (A^0, X) and (DAP) is gradually quenched above 100 K and 30 K, respectively. It is also found that the (A^0, X) peaks move to lower energies and their FWHM values increase with increasing temperature. The (A^0, X) peak shift is due to the shrinkage of the bandgap energy with increasing temperature while the FWHM increases dependent on the exciton scattering process.

The logarithms of the integrated luminescence intensity for the (A^0, X) are plotted versus inverse temperature in Fig. 3. The best fit of the temperature dependence of the bound exciton luminescence (A^0, X) intensity exhibits a two-step-quenching process as described by the following expression [20],

$$I(T) = \frac{I(0)}{[1 + C_1 \exp(-E_1/kT) + C_2 \exp(-E_2/kT)]} \quad (1)$$

where $I(T)$ represents the integral intensity of the bound exciton at different temperatures, $I(0)$ represents the theoretical integral intensity at 0 K, C_1 and C_2 are constants, and E_1 and E_2 are the thermal activation energies in the low- and high-temperature quenching processes, respectively. The temperature dependence of the (A^0, X) is well expressed by this formula with the parameters, E_1 = 5.3 meV, E_2 = 45.8 meV. Actually, the bounding energy of an exciton to acceptor of $Cd_{1-x}Mn_xTe$ is considered to obey the Haynes's rule [21],

$$\frac{E_{BA}}{E_A} = 0.1 \quad (2)$$

where E_{BA} is the binding energy of an exciton to acceptor, and E_A is the ionization energy of acceptor impurities. When the acceptors in CMT have ionization energies of ~60 meV as in CdTe crystal [22], the exciton binding energy E_{BA} is therefore ~6 meV, quite matched with the PL quenching result E_1. According to these results, we can

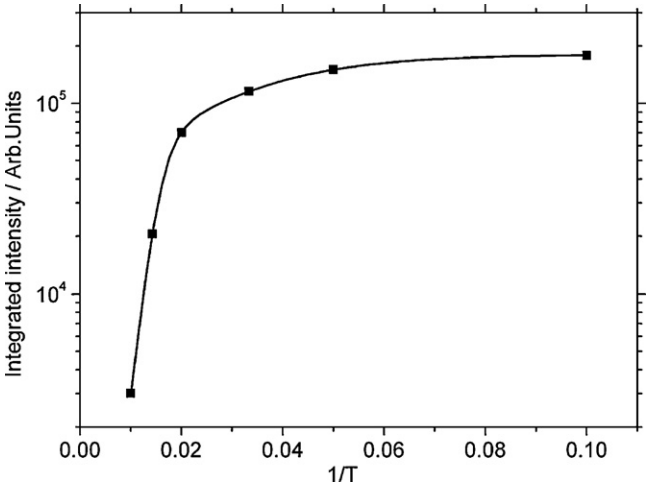

Fig. 3. Temperature dependence of the integrated intensity for the (A^0, X) in the PL spectrum of $Cd_{0.8}Mn_{0.2}Te$. The solid lines are fitting results by Eq. (1).

certainly attribute E_1 as the dissociation energy of excitons from (A^0, X) levels to free exciton (FE) levels at the low temperature. About the activation energy in high-temperature E_2, the integrated intensity I quickly decreased, indicating the presence of nonradiative recombination mechanisms. Bimberg et al. [20] proposed four different general processes for the dissociation of a (A^0, X) system in GaAs, which can be introduced to our system. The dissociation processes are described as

$$(A^0, X) \rightarrow A^0 + X, \qquad E_{Ta} = E(A^0, X) = E_{BA} = 5.3\,\text{meV}, \tag{a}$$

$$(A^0, X) \rightarrow A^0 + h + e, \qquad E_{Tb} = E_{BA} + E_X = 5.3 + 10 = 15.3\,\text{meV}, \tag{b}$$

$$(A^0, X) \rightarrow (A^-, X) + h, \qquad E_{Tc} = E_{Tb} - E(A^0, h) = 15.3 - E(A^0, h), \tag{c}$$

$$(A^0, X) \rightarrow A^- + h + e + h, \qquad E_{Td} = E_{Tb} + E_A = 15.3 + E_A, \tag{d}$$

where process (a) represents a dissociation resulting in a free exciton, process (b) represents a dissociation resulting in one free electron and one free hole, process (c) represents a dissociation resulting in one free hole, and process (d) represents a dissociation resulting in two free holes and one free electron. The binding energy of the bound exciton E_{BA} and the free exciton E_X are 5.3 meV and 10 meV as in CdTe, respectively. When E_2 is 45.8 meV, process (d) is the only possible explanation for the quenching of (A^0, X). The value of E_A is the acceptor ionization energy and supposed to be 30.5 meV. One can therefore conclude that the Auger recombination dominates the dissociation of the (A^0, X) for CMT samples at the high temperature.

Fig. 4 is a plot of the (A^0, X) peak energy position versus the temperature. Assuming the free exciton binding energy is about 10 meV, which is the free exciton binding energy in CdTe, the (A^0, X) peak lies at 15.3 meV below the bandgap energy. The position of (A^0, X) peak at 300 K for CMT was predicted to be at 1.7759 eV by using the equation $E_g = 1.528 + 1.316x_{Mn}$ [23], and added in Fig. 4. The solid line is the curve fit of the temperature variation of (A^0, X) peak using the Varshni expression [24]. The fitting result is

$$(\text{eV})E_{AX} = 1.8847 - \frac{4.8 \times 10^{-4} T^2}{93.36 + T} \tag{3}$$

Therefore the following relationship between the bandgap energy of CMT and temperature can be derived:

$$(\text{eV})E_g = 1.9000 - \frac{4.8 \times 10^{-4} T^2}{93.36 + T} \tag{4}$$

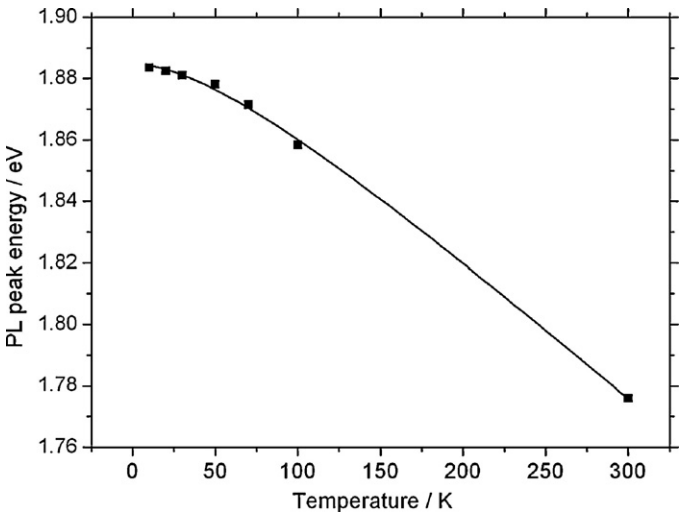

Fig. 4. A plot of the (A^0, X) peak energy position versus the temperature for $Cd_{0.8}Mn_{0.2}Te$. The solid line is the curve fit to the data using the Varshni expression.

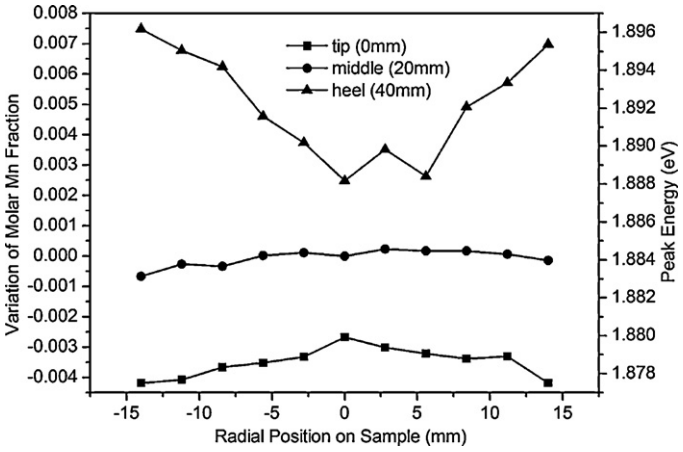

Fig. 5. The radial and axial variation of Mn concentration for a (1 1 1) face $Cd_{0.8}Mn_{0.2}Te$ sample as shown in Fig. 1.

This equation can be used to identify the shrinkage of the bandgap energy with increasing temperature for CMT.

PL spectra at 10 K were taken at various points on the (1 1 1) face sample as shown in Fig. 1 to characterize the composition uniformity; all points were qualitatively similar for the sample. Fig. 5 shows the position of the (A^0, X) peak vs. distance from the radial and axial directions of the sample. Since the (A^0, X) peak lies at 15.3 meV below the bandgap energy, we used the bandgap value at 4.2 K, [1.606 + 1.59x] eV to approximately conduct the Mn concentration variation of the sample within $30 \times 40\,\text{mm}^2$ area [25]. It can be seen that the variation of Mn concentration is within 0.012 mole fraction, which prove a high composition uniformity of the wafer. Meanwhile, the position of the (A^0, X) peak shows a slight shift toward higher energy as one moves to the heel of the ingot, indicating the segregation coefficient of Mn is close to unit. The homogeneity of the CMT wafer is beneficial for the detector performance, since the bandgap and the average atomic number of the material is stable, as well as the defects are reduced [26].

4. Conclusion

The temperature-dependent photoluminescence spectroscopy was adopted to characterize $Cd_{0.8}Mn_{0.2}Te$ crystals grown by the vertical Bridgman method, which revealed the neutral acceptor bound exciton (A^0, X) peak and the donor–acceptor pair (DAP) peak. The low values of the FWHM of (A^0, X) peaks and the defect radiative density indicated a high crystal quality of the as-grown $Cd_{0.8}Mn_{0.2}Te$ crystal. The activation energies derived from the PL quenching of the (A^0, X) peak was estimated to be 5.3 meV and 45.8 meV, suggesting the binding energy of excitons to acceptors at lower temperatures and the Auger recombination at higher temperatures. Therefore, the temperature dependence of bandgap energy E_g for $Cd_{0.8}Mn_{0.2}Te$ from 10 K to 300 K was first established. The PL spectra with the (1 1 1) face $Cd_{0.8}Mn_{0.2}Te$ plates ($30 \times 40\,\text{mm}^2$ area) indicated that the variation of Mn concentration is within 0.012 mole fraction, which proved that homogeneous $Cd_{0.8}Mn_{0.2}Te$ crystals can be grown from the vertical Bridgman method.

Acknowledgements

This work was supported by the National Natural Science Foundations of China (No. 50902091), Shanghai Postdoctoral Scientific Program (No. 09R21413000), Program for Changjiang Scholars Innovative Research Team in University (No: IRT0739), and Shanghai Leading Academic Disciplines (S30107).

References

[1] J.K. Furdyna, J. Appl. Phys. 64 (1988) R29.
[2] A. Mycielski, L. Kowalczyk, R.R. Galazka, R. Sobolewski, D. Wang, A. Burger, M. Sowinska, M. Groza, P. Siffert, A. Szadkowski, B. Witkowska, W. Kaliszek, J. Alloy Compd. 423 (2006) 163.
[3] G.A. Brost, K.M. Magde, S. Trivedi, Opt. Mater. 4 (1995) 224.
[4] A.G. Podoleanu, R.G. Cucu, D.A. Jackson, Proc. SPIE 4068 (2000) 615.
[5] A. Burger, K. Chattopadhyay, H. Chen, J.O. Ndap, X. Ma, S. Trivedi, S.W. Kutcher, R. Che, R. Rosemeier, J. Cryst. Growth 198/199 (1999) 872.
[6] A. Hossain, Y. Cui, A.E. Bolotnikov, G.S. Camarda, G. Yang, D. Kochanowska, M. Witkowska-baran, A. Mycielski, R.B. James, J. Electron. Mater. 38 (2009) 1593.
[7] A. Mycielski, A. Burger, M. Sowinska, M. Groza, A. Szadkowski, P. Wojnar, B. Witkowska, W. Kaliszek, P. Siffert, Phys. Status Solidi (c) 2 (2005) 1578.
[8] P. Fougeres, L. Chibani, M. Hageali, J.M. Koebel, G. Hennard, A. Zumbiehl, P. Siffert, M. Benkaddour, J. Cryst. Growth 197 (1999) 641.
[9] R. Triboulet, A. Heurtel, J. Rioux, J. Cryst. Growth 101 (1990) 131.
[10] M. Azoulay, A. Raizman, R. Weingarten, H. Shacham, H. Feldstein, J. Cryst. Growth 128 (1993) 588.
[11] S.B. Trivedi, C.C. Wang, S. Kutcher, U. Hommerich, W. Palosz, J. Cryst. Growth 310 (2008) 1099.
[12] H. Sato, K. Onodera, H. Ohba, J. Cryst. Growth 214/215 (2000) 885.
[13] G.Q. Li, X.L. Zhang, W.Q. Jie, Semicond. Sci. Technol. 20 (2005) 86.
[14] W. Stadler, D.M. Hofmann, H.C. Alt, T. Muschik, B.K. Meyer, E. Weigel, G. Müller-Vogt, M. Salk, E. Rupp, K.W. Benz, Phys. Rev. B 51 (1995) 10619.
[15] J.E. Toney, B.A. Brunett, T.E. Schlesinger, J.M. Vanscyoc, R.B. James, M. Schieber, M. Goorsky, H. Yoon, E. Eissler, C. Johnson, Nucl. Instrum. Methods Phys. Res. A 380 (1996) 132.
[16] D. Heiman, P. Becla, R. Kershaw, D. Ridgley, K. Dwight, A. Wold, R.R. Galazka, Phys. Rev. B 34 (1986) 3961.
[17] M.P. Vecchi, W. Giriat, L. Videla, Appl. Phys. Lett. 38 (1981) 99.
[18] H.Y. Shin, C.Y. Sun, Mater. Sci. Eng. B 52 (1998) 78.
[19] P.Y. Tseng, C.B. Fu, M.C. Kuo, C.S. Yang, C.C. Huang, W.C. Chou, Y.T. Shih, H.Y. Hsin, S.M. Lan, W.H. Lan, Mater. Chem. Phys. 78 (2002) 529.
[20] D. Bimberg, M. Sondergeld, E. Grobe, Phys. Rev. B 4 (1971) 3451.
[21] J.R. Haynes, Phys. Rev. Lett. 4 (1960) 361.
[22] E. Molva, J.L. Pautrat, K. Saminadayar, G. Milchberg, N. Magnea, Phys. Rev. B 30 (1984) 3344.
[23] Y.R. Lee, A.K. Ramdas, Solid State Commun. 51 (11) (1984) 861.
[24] Y.P. Varshni, Physica 34 (1) (1967) 149.
[25] Y.H. Matsuda, T. Ikaida, N. Miura, S. Kuroda, F. Takano, K. Takita, Phys. Rev. B 65 (2002) 115202.
[26] T.E. Schlesinger, J.E. Toney, H. Yoon, E.Y. Lee, B.A. Brunett, L. Franks, R.B. James, Mater. Sci. Eng. R 32 (2001) 103.